

# STRUCTURAL, MECHANICAL, OPTICAL, THERMAL, ELECTRICAL STUDIES OF A NONLINEAR OPTICAL SINGLE CRYSTAL: GAMMA GLYCINE USING LITHIUM BROMIDE AS AN ADDITIVE

K. Lilly Mary Eucharista\*, C. Krishnan\*\* & P. Selvarajan\*\*\*

\* Department of Physics, Sri Meenakshi Government Arts College for Women (Autonomous), Madurai, Tamilnadu

\*\* Department of Physics, Arignar Anna College, Aralvoymoli, Tamilnadu \*\*\* Department of Physics, Aditanar College of Arts and Science, Tiruchendur, Tamilnadu

**Cite This Article:** K. Lilly Mary Eucharista, C. Krishnan & P. Selvarajan, "Structural, Mechanical, Optical, Thermal, Electrical Studies of a Nonlinear Optical Single Crystal: Gamma Glycine Using Lithium Bromide as an Additive", International Journal of Advanced Trends in Engineering and Technology, Volume 2, Issue 2, Page Number 60-70, 2017.

## Abstract:

Single crystals of gamma glycine, an organic nonlinear optical material were grown by slow evaporation method from aqueous solutions of lithium bromide. Good optical quality single crystals were grown within a period of 3 weeks. The grown crystals were colorless and transparent. The solubility of the grown crystals has been estimated for various temperatures. The XRD study reveals that the grown crystal crystallizes in the hexagonal crystal system and corresponding lattice parameters were determined. The reflection planes of the sample were confirmed by the powder X-ray diffraction study and diffraction peaks were indexed. Fourier transform infrared (FTIR) study was used to confirm the presence of various functional groups in the grown crystal. The optical spectral analysis of the grown crystal has been performed by UV-Vis-NIR spectroscopy and the band gap energy was found out. Second harmonic generation (SHG) for the materials of this work was confirmed using Nd:YAG laser. The thermal stability of the crystal was studied by thermo gravimetric analysis (TGA) and differential thermal analysis (DTA). The dielectric constant and the dielectric loss were measured for varying frequencies under different temperatures. The impedance measurements were performed as a function of temperature.

**Key Words:** Crystal Growth, Growth from Solutions, Nonlinear Optical Material & Characterization **1. Introduction:** 

The synthesis of novel and efficient frequency conversion materials has resulted in the development of semi organic materials, which possess large nonlinearity, high resistance to laser induced damage, low angular sensitivity and good mechanical stability [1, 2]. Amino acids are interesting organic materials for NLO applications as they contain zwitterions, which create hydrogen bonds. Amino acids have two or more types of coordination atoms and can act as various bridging ligands [3, 4]. Amino acids and their complexes belong to a family of organic materials that have been considered for photonic applications [5]. Photonic crystals which prohibit the propagation of light for frequencies within a band gap, have enabled exciting new ways to control light and construct integrated optical devices. Glycine is the simplest amino acid. Unlike other amino acids, it has no asymmetric carbon atom and is optically inactive. It has three polymeric crystalline forms  $\alpha$ ,  $\beta$  and  $\gamma$  [6-8]. The α-form of glycine crystallizes in centrosymmetric structure hence it does not exhibit second harmonic generation, whereas  $\beta$  and  $\gamma$  forms crystallizes in noncentrosymmetric crystal structure. The  $\beta$ - form of glycine is unstable. The  $\gamma$ - form of glycine exhibit second harmonic generation and the conversion efficiency is reported to 1.5 times greater than that of KDP [9]. Some complexes of glycine with inorganic salts are Lithium Sulphate [10], Sodium Nitrate [11], Potassium Sulphate [12], and Zinc Chloride [13] that forms NLOsemiorganic crystals. The present paper deals with the growth of gamma-glycine by slow evaporation technique and characterization by single crystal X-ray Diffraction (XRD), Fourier Transform Infrared (FTIR) spectrum, UV analysis, NLO, Thermal studies and microhardness test.

#### 2. Experimental Methods:

**2.1 Synthesis and Solubility:** The title compound was synthesized by taking precursor chemicals like AR grade Glycine and Lithium Bromide in the molar ratio 2:1 by slow evaporation method. Calculated amounts of the chemicals were dissolved in water solvent and the salt was synthesized and it was re-crystallized twice. The solubility study of the title compound in aqueous solution was performed using a hot-plate magnetic stirrer and a digital thermometer by the gravimetric method [14, 15]. The re-crystallized salt of gamma-glycine was added step by step to 25 ml of water in an air tight container kept on the hot-plate magnetic stirrer. Addition of the salt and stirring were continued till a small precipitate was formed. This gave the conformation of the supersaturated condition of the solution. Then 10ml of the clear liquid was withdrawn by means of pipette and the same was poured into a clean, dry and weighed empty Petri dish. The solution was warmed up at 45°C till the solvent was completely evaporated out. The amount of salt present in the 10 ml of the solution was measured by subtracting the weight of the empty Petri dish. From this, the quantity of gamma-glycine salt (in gram) dissolved in 100 ml of water was determined. The same procedure was followed to find out the solubility of gamma-glycine sample

for various temperatures. The solubility curve of gamma-glycine is shown in Fig.1. From the curve, it is observed that the solubility of gamma-glycine sample in water linearly increases with temperature, exhibiting a high solubility gradient and positive temperature coefficient. This shows the slow evaporation technique is the appropriate method and the solvent is suitable for the growth of gamma-glycine crystal.

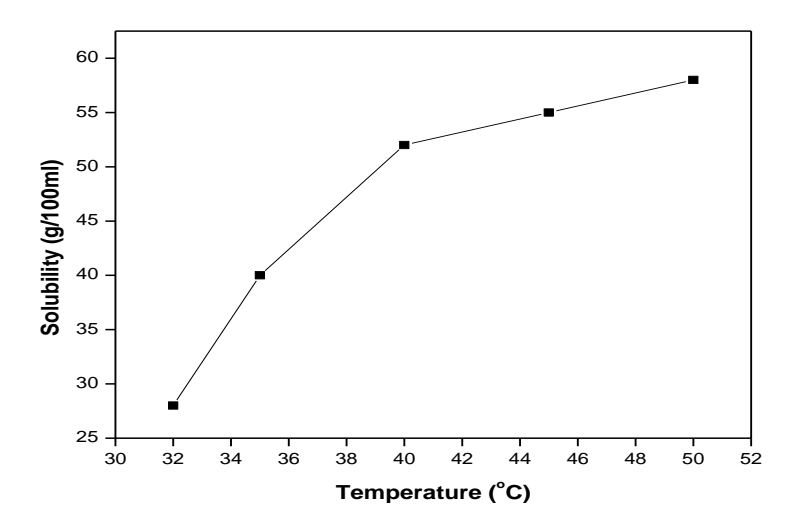


Figure 1: Solubility Curve of Gamma-Glycine Crystal

**2.2 Crystal Growth:** In order to grow single crystal of gamma-glycine in accordance with the solubility data, saturated solution was prepared and it was continuously stirred about two hours to ensure homogeneous concentration and temperature throughout the volume of the solution. Then the solution was filtered using a high quality 4micron Whatmann filter paper to remove extraneous solid colloidal particles. To obtain big single crystals, the bottom seed growth tecnique was adopted. The prepared saturated solution was taken in a beaker and covered by perforated cover for controlled evaporation and kept in a undisturbed condition. The seed crystals of gamma-glycine were obtained by spontaneous nucleation. The supersaturation of the solution was found by observing the first crystal formed at the bottom of the glass beaker due to slow evaporation of the solvent. The super saturated solution of gamma-glycine was transferred into another beaker and kept at room temperature. The defect-free seed crystals were placed in the supersaturated solution and the solution was allowed to evaporate. Good quality of stable, transparent and colorless crystals was harvested within a period of 2 weeks. The size of the grown crystal is 7 x 5 x 3 mm³. The photograph of the grown crystal is displayed in Figure 2.

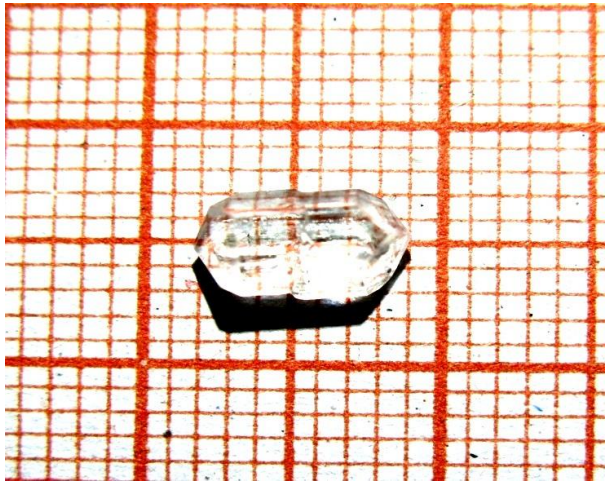


Figure 2: Photograph of gamma-glycine crystal

## 3. Characterization Techniques:

The grown crystal of gamma-glycine was subjected to the following characterization studies. The single crystal X-ray diffraction was performed using ENRAF NONIUS CAD-4 Xray diffractometer. The grown gamma-glycine crystal has been crushed into fine powder and subjected to powder XRD study using a XPert Pro Powder X-ray diffractometer with CuK $\alpha$  radiation ( $\lambda$ =1.54056Å). The sample was scanned in the 2 $\theta$  values ranging from 10° to 80°. The optical transmission spectrum of gamma-glycine crystal was recorded using a UV-Vis-NIR spectrophotometer(Lambda 35 model)from 190 to 1100nm. A Perkin Elmer FTIR spectrometer was used for IR spectral measurements. The sample was prepared by the KBr pellet tecnique and the spectrum was

rcorded in the range of  $4000\text{-}400\text{cm}^{-1}$ . The gamma-glycine crystal was tested for the microhardness property using a Vickers microhardness tester with diamond indenter. The dielectric constant ( $\epsilon_r$ ) and the dielectric loss(tan $\delta$ ) of gamma-glycine crystal of known dimension were carried out using a precision LCR meter with frequency range of 10 to 100 Hz at different temperatures ranging from 308-373 K. The thermogravimetric analysis and differential thermal analysis (TG/DTA) curves were recorded by employing Perkin Elmer thermal analyzer in nitrogen atmosphere at a heating rate of  $10^{\circ}\text{C/min}$ . and the temperature from  $40^{\circ}\text{C}$  to  $750^{\circ}\text{C}$  for the grown crystal. The SHG test for the grown gamma-glycine crystals was performed by the powder technique of Kurtz and Perry[16]. Bulk resistance and dc conductivity of the grown crystal were determined from Nyquist plot.

#### 4. Results and Discussion:

**4.1 X-Ray Diffraction Studies:** Single crystal X-ray diffractometric analysis reveals that gamma-glycine crystal belongs to the hexagonal system which is recognized as non-centrosymmetric and thus satisfying one of the basic and essential requirements for the SHG activity of the crystal. The lattice parameter values are a=b=7.018(3)Å, c=5.471(6)Å,  $\alpha=\beta=90^{\circ}$ ,  $\gamma=119.90^{\circ}$  and volume=234.3(1)Å<sup>3</sup>. Powder XRD study was also carried out to check the correctness of the data and to identify the diffraction planes of grown crystal. Powder XRD pattern of gamma-glycine crystal is shown in Fig.3. The sharp Bragg peaks of powder XRD pattern were indexed using the TREOR software package following the procedure of Lipson and Steeple[17]. Specific well-defined peaks at  $2\theta$  values indicate high crystallinity of the grown crystal.

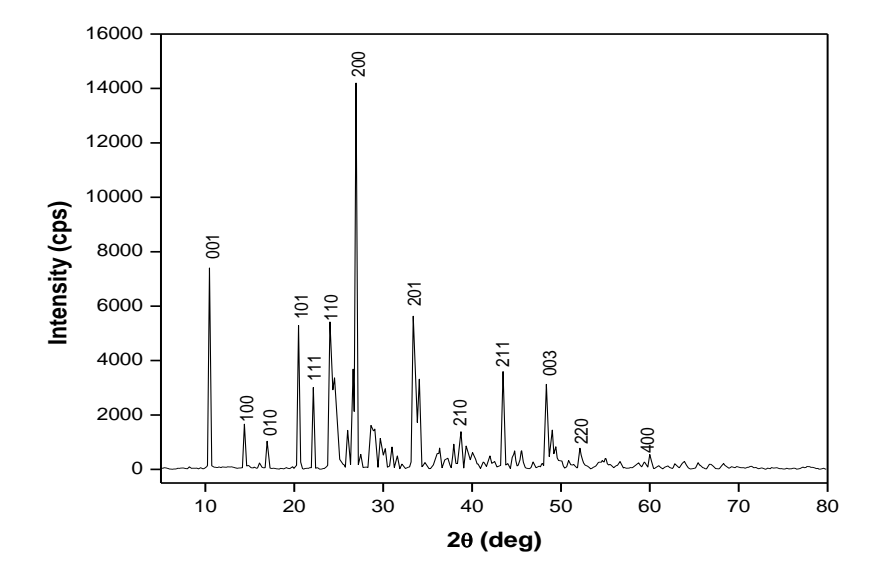


Figure 3: Powder X-ray diffraction pattern of gamma-glycine crystal

**4.2 Fourier Transform Infrared Analysis:** The functional groups of gamma-glycine crystals involved in vibration frequency have been identified using FTIR spectroscopy. The grown gamma-glycine FTIR spectrum was taken between wave number 400cm<sup>-1</sup> and 4000 cm<sup>-1</sup>. The recorded spectrum is shown in fig 4

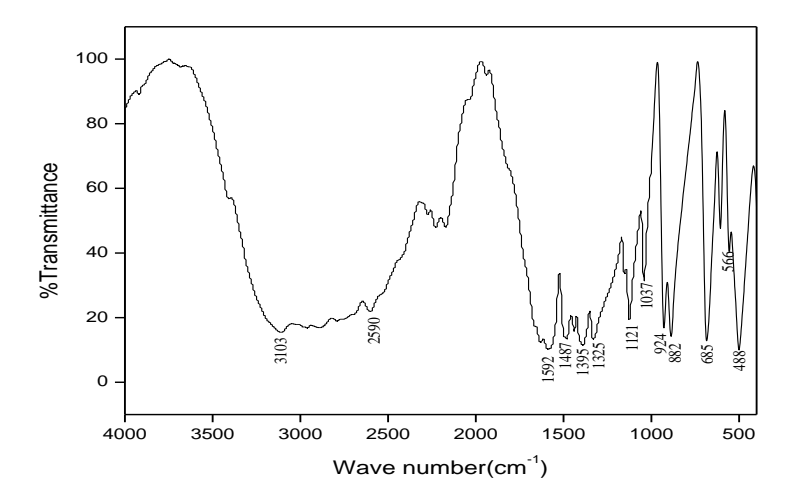


Figure 4: FTIR Spectrum of Gamma-Glycine Single Crystal

Glycine exists as zwitterions in which the carboxyl group present as carboxylate ion and the amino group exist as ammonium ion. Transmission is due to the carboxylate group of free glycine. The stretching type of vibrations of hydrogen bond gives rise to several bands in the region of  $3110\text{-}2604\text{cm}^{-1}$  inthe FTIR spectrum. The transmission peaks for the NH $_3^+$  group of free glycine are observed at 3175,2614,1507 and  $1110\text{cm}^{-1}$  respectively [18]. In gamma-glycine system, NH $_3^+$  group of free glycine are shifted to 3110,2604,1592 and  $1121\text{ cm}^{-1}$  respectively. Peak at  $2155\text{ cm}^{-1}$  is due to the combination of NH $_3^+$  asymmetric stretching and torsional oscillation. Peaks at 1487,1374,1044,938,679 and  $496\text{ cm}^{-1}$  are attributed to CH $_2$ , C-O-O, C-N,CH $_2$ ,C-O-O and C-C-O groups respectively.

Table 1: Comparison of FTIR bands of gamma-glycine with Glycine

Wave number (cm <sup>-1</sup> )		Accionments	
Glycine	Gamma-Glycine	Assignments	
3175	3110	NH <sub>3</sub> <sup>+</sup> stretching	
2614	2604	CH stretching	
2122	2155	Combination of NH <sub>3</sub> <sup>+</sup> asymmetric stretching and torsional oscillation	
1507	1592	NH <sub>3</sub> <sup>+</sup> symmetric bending	
1445	1487	CH <sub>2</sub> bending	
1333	1374	C-O-O symmetric stretching	
1110	1121	NH3 <sup>+</sup> rocking	
1033	1044	C-N stretching	
910	938	CH <sub>2</sub> rocking	
694	679	C-O-O bending	
504	496	C-C-O bending	

**4.3 Optical Property:** The transmission range and cut-off wavelength of single crystals are important factors for optical applications. To find the transmission range of gamma-glycine, the optical transmission spectrum of the gamma-glycine for the wavelength between 190 and 1100nm was recorded using Perkin Elmer Lambda UV-Vis-NIR spectrometer. The transmittance spectrum of gamma-glycine crystal is shown in Fig. 5.

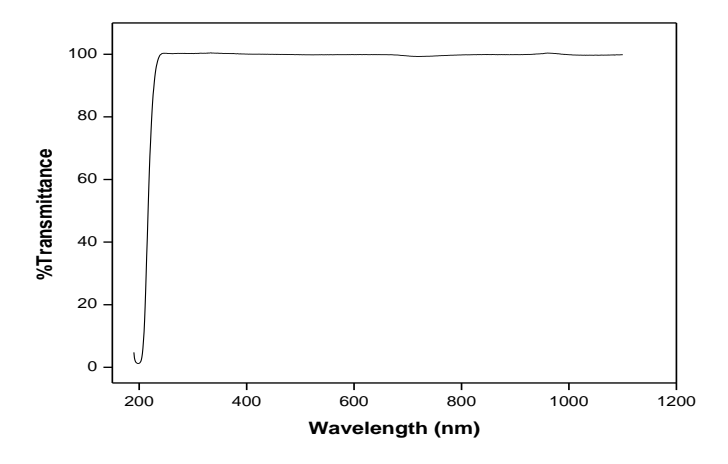
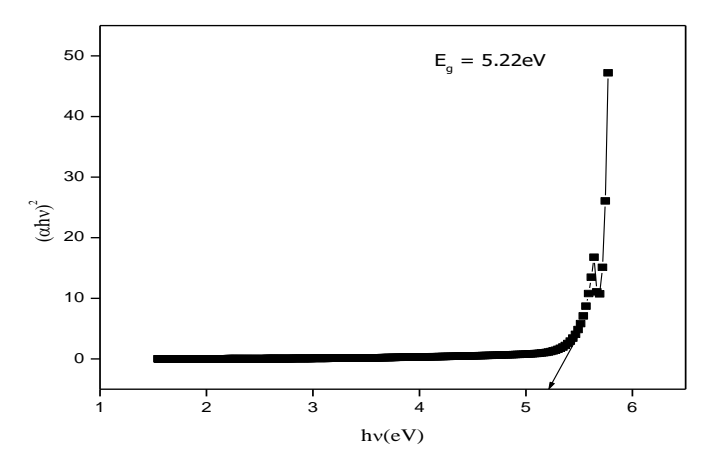


Figure 5: UV-Vis-NIR spectrum of gamma-glycine crystal



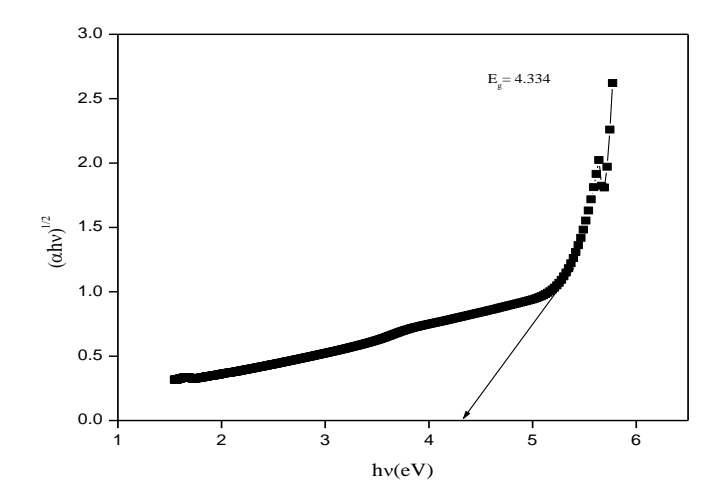


Figure 6: Plot of (a)  $(\alpha hv)^2$  versus hv giving direct band gap (b)  $(\alpha hv)^{1/2}$  versus hv giving indirect band gap

The transmission for entire visible region with the lower cut-off wavelength at 241nm suggests that the material is quite suitable for SHG generation and other related optoelectronic applications. The good transmission of the crystal in the entire visible region suggests the suitability of the grown crystal for second harmonic device fabrication [19].

The dependence of optical absorption coefficient on photon energy helps to study the band structure and the type of transition of electrons. The optical absorption coefficient ( $\alpha$ ) was calculated from transmittance using the following relation,

$$\alpha = \frac{1}{d} \log (1/T) \tag{1}$$

Where **T** is the transmittance and d is the thickness of the crystal.

The optical band gap of the gamma-glycine single crystal was determined from the absorption spectrum using the near-band edge absorption relation,

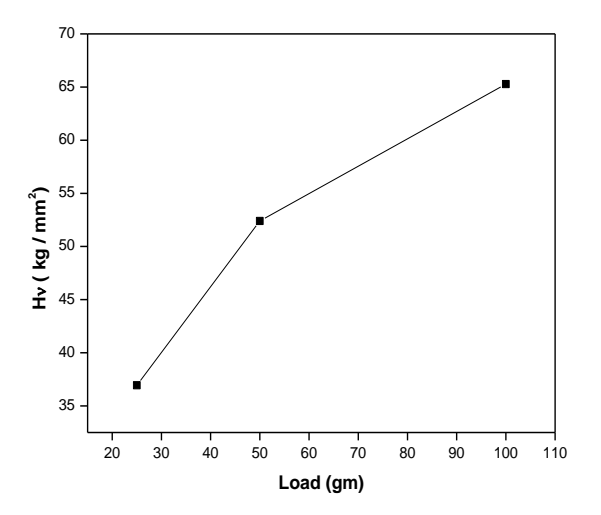
$$(\alpha h \nu)^{n} = A(h \nu - E_{g}) \tag{2}$$

Where A-the optical transition dependent constant,  $E_g$ — optical energy band gap,  $\nu$  — the frequency of incident beam, h- Planck's constant, n- characterizes the transition. For direct allowed and forbidden transitions, n=2 and 2/3 respectively, and n=1/2 and 1/3 for indirect allowed and forbidden transitions respectively.

The analysis of equation (2) showed that, n=2 and  $\frac{1}{2}$  fitted for the as grown gamma-glycine single crystals sample confirming direct and indirect allowed transition. Figure 6(a) and 6(b) shows the plot of  $(\alpha h v)^2$  against hv and  $(\alpha h v)^{1/2}$  against hv respectively for gamma-glycine crystals. The intercept of the straight line on the photon energy axis gives the direct band gap value 5.22eV and indirect band gap value 4.334 eV.

- **4.4 Second Harmonic Generation Test:** Second harmonic generation (SHG) is also called a frequency doubling in nonlinear optics in which photons interacting with a nonlinear material are effectively combined to form new study of NLO efficiency has been carried out by modified experimental set up of Kurtz and Perry [20]. The crystal was grind into a homogenous powder and densely packed between two transparent glass micro capillary tubes. An intensity of Nd: YAG laser(λ=1064nm) with input pulse of 1.9mJ was passed through an IR reflector and then directed on the micro crystalline powdered sample packed in a capillary tube. The SHG behavior was confirmed from the output of the laser beam having green light emission. The second harmonic output signal of 50 mV was obtained for gamma-glycine crystal. The output signal obtained for the reference material was 75 mV for the same input pulse of 1.9 mJ. Thus the relative measured output from the sample with respect to KDP crystal shows that SHG efficiency of the gamma-glycine crystal is 0.633 times as that of the KDP crystal. Thus the grown gamma-glycine sample has good NLO property.
- **4.5 Vickers Micro Hardness Test:** Micro hardness testing is one of the best methods for understanding the mechanical behavior of the materials such as brittleness, yield strength, fracture behavior and cracking temperature [21, 22]. Micro hardness analysis was carried out using Vickers micro hardness tester fitted with a diamondindenter. A well-polished gamma-glycine crystal of 1.5mm thickness was placed on the platform of Vickers micro hardness tester and the loads of different magnitude were applied over fixed interval of time. The micro hardness number ( $H_v$ ) can be calculated using the formula  $H_v$ =1.8544P/d² kg/mm², where P is the load applied in grams and d is the diagonal length of the indentation impression in millimeter [23]. The relation between hardness number ( $H_v$ ) and load (P) for gamma-glycine is shown in Fig.8. According to the normal Indentation Size Effect (ISE), the micro hardness number of a crystal decreases with increasing load and according to the Reverse Indentation Size Effect (RISE), the hardness number of a crystal increases with increase in load up to

100g, further increase in load create the cracks on the surface of the crystal due to the release of internal stresses produced by indentation [26].



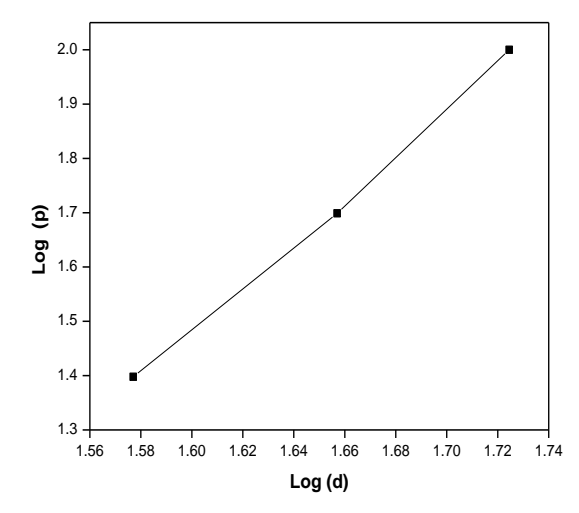


Figure 7: Variation of hardness number with load for gamma-glycine crystal

Figure 8: Plot of log(P) versus log(d) for gammaglycine crystal

The relation between the load and size of indentation is given by Mayer's law P=ad<sup>n</sup>, where n is the work hardening coefficient or Mayer's index, d is the recovered indentation in mm,a is a constant and P is the load [27]. The plot of log(P) against log(d) is a straight line, which is shown in Fig.8. The slope of the straight line gives the work hardening coefficient(n). The work hardening coefficient for the grown crystal is found to be 4.0723. From careful observations on various material, Onitsch pointed out that for hard materialsn lies between 1 and 1.6 and for soft materials it is above 1.6 [28]. Based on the above fact, it is obvious that gammaglycine crystal belongs to soft material category.

**4.6 TG/DTA Analysis:** The thermo gravimetric analysis (TGA) and the differential thermal analysis (DTA) give information regarding phase transition and different stages of decomposition of the crystal system [29]. The TG/DTA curves for gamma-glycine crystal were recorded for the range of temperature from 40-750°C in nitrogen atmosphere at the heating rate of 10°C/min using the instrument Perkin Elmer STA 6000 thermal analyzer. The initial mass of the material was taken to be 9.460mg. The thermo gravimetric analysis and differential thermal analysis (TG/DTA) of gamma-glycine crystal are displayed in Fig.9. The sample is stable upto 233°C. The grown crystal gamma-glycine exhibits a single stage of decomposition. The first weight loss occurs at 233°C. The decrease in mass may be due to the thermal decomposition of elements present in the sample. The mass changes in the TG curve are confirmed by DTA peaks shown in figure Fig.9. This shows that the grown crystal is thermally stable and makes it suitable for possible applications in lasers where the crystal is required to withstand high temperatures.

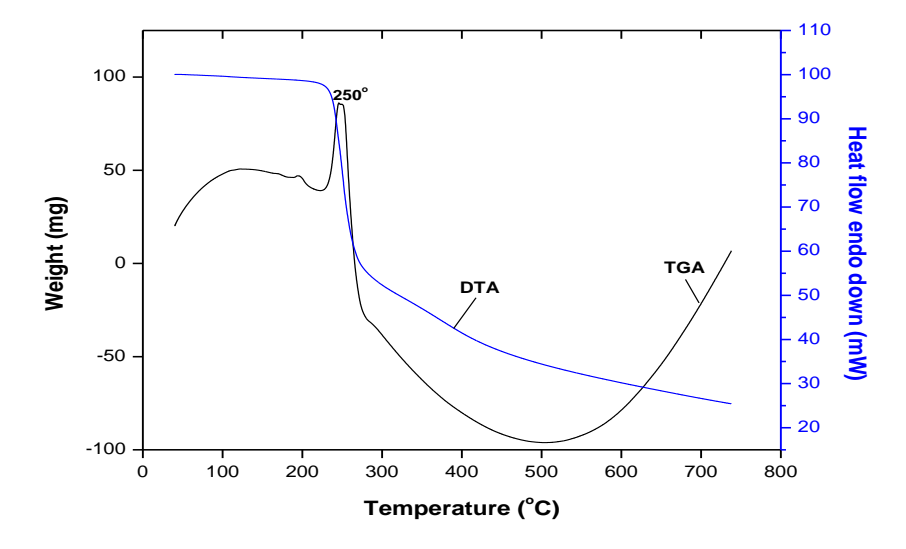
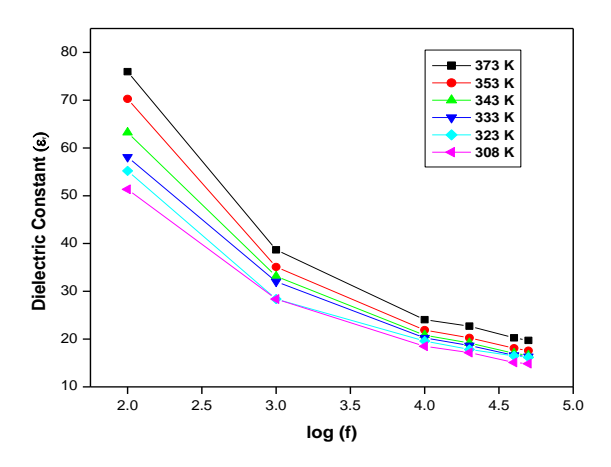


Figure 9: TGA/DTA curves for gamma-glycine crystal

**4.7 Dielectric Studies:** Crystals with high transparency and large defect-free size were selected and used for the dielectric measurements. The dielectric constant ( $\varepsilon_r$ ) and the dielectric loss (tan  $\delta$ ) were measured for varying frequencies ( $10^2$  - $10^6$  Hz) under different temperatures (35- $100^{\circ}$ C). The observations were made while cooling the samples. The values of dielectricconstant ( $\varepsilon_r$ ) and the dielectric loss (tan $\delta$ ) are found to be increases with increase in temperature and decreases with increase in frequency(Fig.10 and 11). This can be explained on the basis of polarizationand conduction processes. The high values of dielectric constant at low frequencies may be due to the presence of all the four polarizations namely space charge, oriental, ionic and electronic polarizations and its low value at high frequencies may be due to the loss of all these polarizations. It is observed that space charge polarization is dominant and electronic and ionic polarizations are not very much active in low frequency region[30, 31]. The low value of dielectric loss (tan  $\delta$ ) at high frequency reveals the high optical quality of the crystals with lesser defects, which is the desirable property for NLO applications [32].



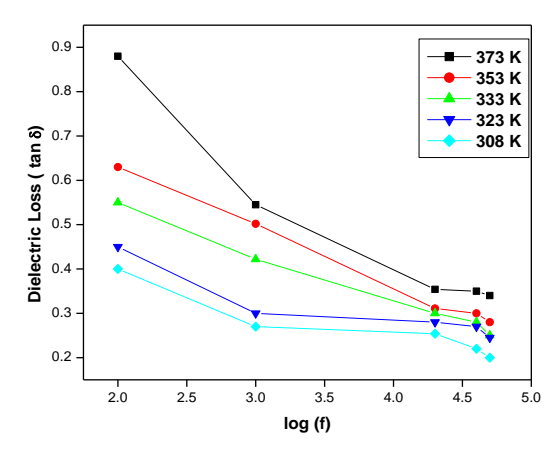
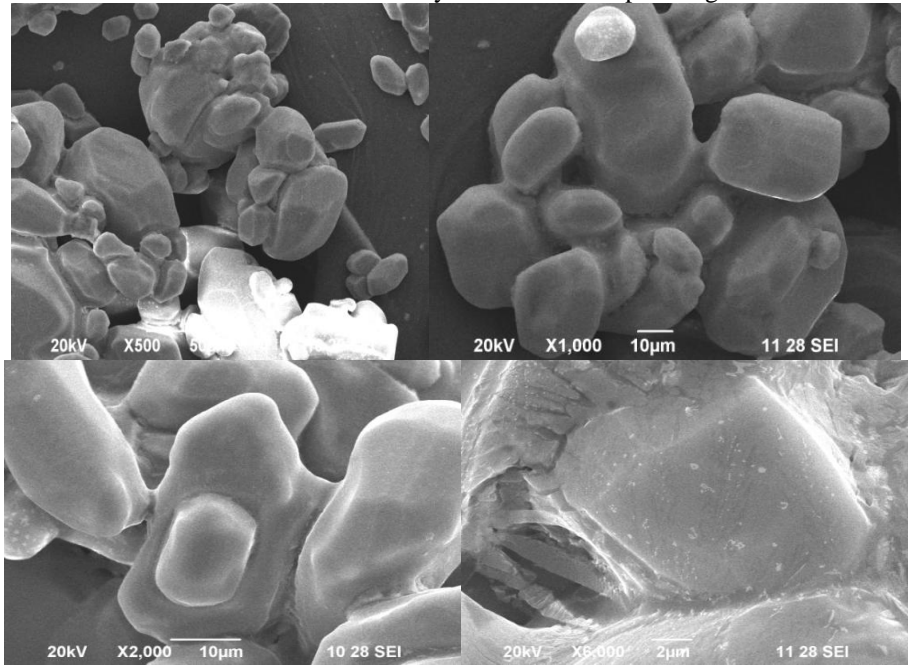


Figure 10: Variation of dielectric constant with frequency for gamma-glycine crystal

Figure 11: Variation of dielectric loss with frequency for gamma-glycine crystal

The increase in dielectric constant ( $\epsilon_r$ ) with temperature is generally attributed to crystal expansion, electronic and ionic polarizations and the presence of crystal defects [33, 34].

**4.8 SEM and EDAX Analysis:** The surface morphology and nature of the grown crystal analysis was studied by scanning electron microscope (SEM) and the image of gamma-glycine is shown in Fig.12. Carbon coating was applied for the sample before subjecting the crystal surface to electron beam to make a non-conductive into conductive specimen. During recording the image through SEM the appropriate coating is necessary to provide good conductivity and for the good emission of secondary electrons. From the Fig.12.It can be observed that the grown crystal has cracks and few inclusions which may be due to the impact of growth conditions.



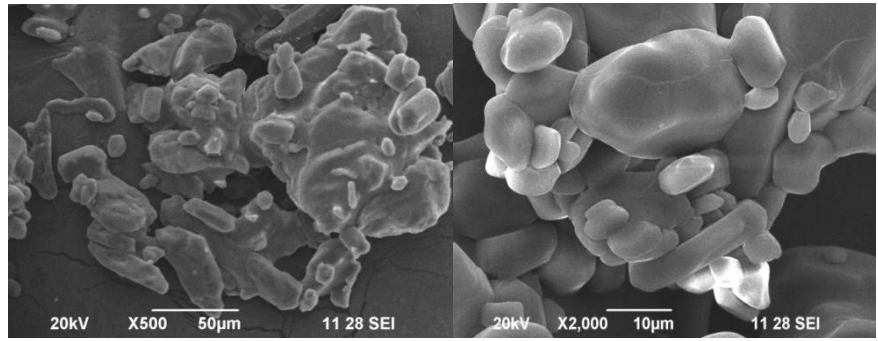


Figure 12: SEM image of gamma-glycine crystal

The crystalline or chemical composition of the grown crystal was examined by energy dispersive X-ray analysis (EDAX) spectrometer. The EDAX spectrum is resulting from the electron back scattering. Further the obtained spectrum of energy versus relative counts of the X-rays gives the qualitative and quantitative information about the elements present in the testing sample. Fig.13. shows the EDAX spectrum of gammaglycine. The weight percentages of O and Br as obtained from EDAX analysis are given in table 2.

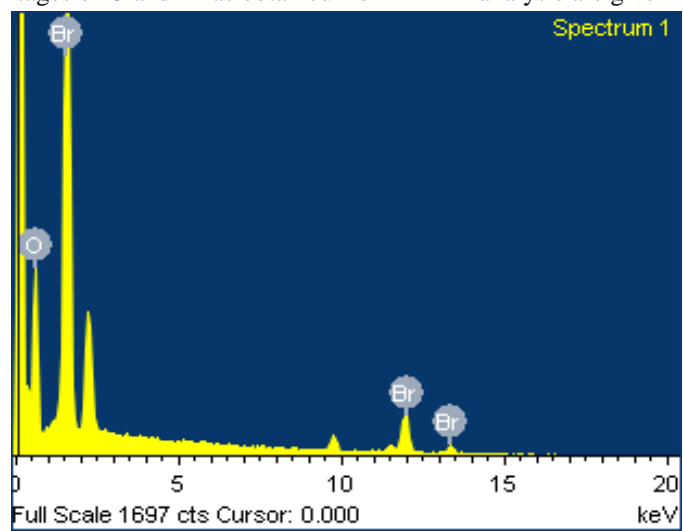


Figure 13: EDAX Spectrum of gamma-glycine crystal Table 2: EDAX Quantification table

Element	Weight %	Atomic %
O K	42.32	78.56
Br L	57.68	21.44
Total	100	100

**4.9 Impedance Analysis:** Complex impedance spectroscopy is a powerful technique to investigate the electrical properties and process of the materials. This technique is based on analyzing the ac response of a system to a sinusoidal perturbation, and subsequent calculation of impedance and related parameters as a function of frequency of the perturbation. The motion of charges could occurs dipole reorientation, space charge formalism and charge displacement. The impedance measurements on a material give us data having both resistive (real part) and reactive (imaginary part) components. The frequency dependent properties (electrical properties) of a material are often represented in terms of complex impedance Z\* and which is related as

$$Z*(\omega) = Z'-jZ''$$

where Z' and Z" are the real and imaginary components of impedance. The complex impedance of the electrode/insulator/electrode capacitor can be demonstrated as the sum of the single RC circuit with parallel combination. In this work, the measurements on impedance of the grown gamma-glycine crystals were carried out using an impedance analyzer (Model: IM 6 ZAHNER/Germany-Electrochemical Workstation) to find the impedance, bulk resistance, grain boundary resistance, DC conductivity and relaxation time of the samples.

The variation of real part of impedance (Z') and the imaginary part of impedance (Z'') with frequencies at temperatures 30, 50, 70 and 90 $^{\circ}$ C are shown in figures 14 and 15.

Fig.14. indicates that the real part of impedance (i.e., resistance) decreases with rise in frequency. This plot provides an indication of increasing conduction with temperature coefficient with temperature and frequency (i.e., negative temperature coefficient of resistance behavior like that of semiconductor). The coincidence of the impedance (Z') at higher frequencies at all the temperature indicates a possible release of space charge [35].

Fig.15. shows the variation of imaginary part of impedance (Z") with frequency at different temperatures. This plot is suitable for evaluation of the relaxation frequency of most resistive contribution. The relaxation frequency can be obtained either from the plot of Z" against frequency or semicircles from the Nyquist plot. The peak broadening on increasing temperature suggests the presence of temperature dependent relaxation processes in the compound [36]. The relaxation process may be due to the presence of immobile species at low temperature and defects at higher temperature.

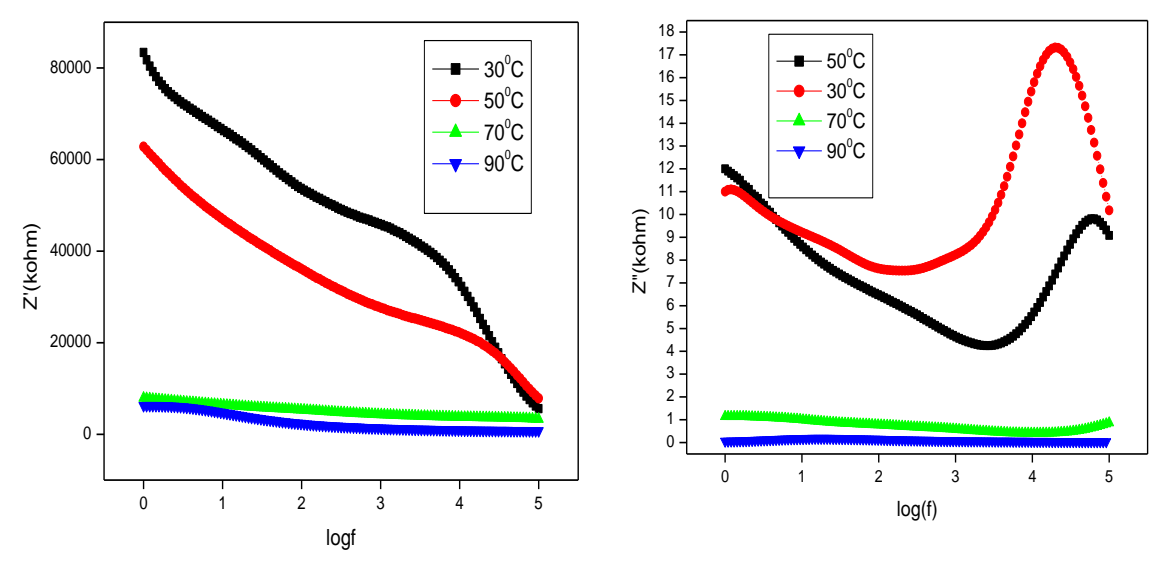


Figure 14: Variation of real part of impedance (Z') as a function of frequency for gamma-glycine crystal

Figure 15: Variation of imaginary part of impedance (Z") as a function of frequency for gamma-glycine crystal

Fig.16. shows the Nyquist plot (complex impedance spectrum) of gamma-glycine crystal at different temperatures and this graph explains the transport response function. From the graph, one partial semicircular arc has been observed and this depicts the bulk effect. This bulk effect arises due to the parallel combination of bulk resistance (Rb). The value of bulk resistance ( $R_b$ ) at different temperatures has been obtained from the intercept of the semicircular arc on the real axis (Z'). These values are given in table 3. From fig.16. It is clear that the value of  $R_b$  decreases with rise in temperature. This shows the negative temperature coefficient of resistivity (NTCR) behavior like that of a semiconductor.

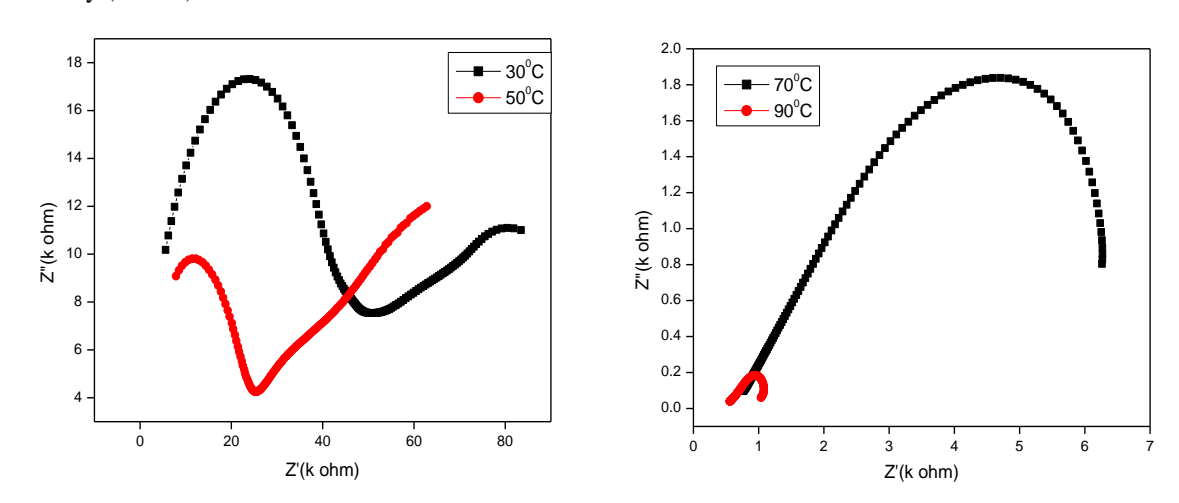


Figure 16: a) Nyquist plot for gamma-glycine crystal (30° &50°) b) Nyquist plot for gamma-glycine crystal (70° & 90°)

Table 3: The value of bulk resistance of gamma-glycine crystal

Temperature (°C)	Bulk resistance $R_b(k\Omega)$
30	51.05
50	25.23
70	6.248
90	1.058

The dc conductivity  $(\sigma_{dc})$  of the crystal is calculated using the formula

$$\sigma_{dc} = d/R_bA$$

Where A is the area of crystal surface and d is the thickness of the crystal. It is observed that the dc conductivity increases with temperature. Fig. 17. shows the variation of  $\sigma_{dc}$  against  $10^3/T$ . The value of bulk conductivity of the material is evaluated from the complex impedance plots of the sample at different temperatures. At higher temperature, the conductivity versus temperature response is more or less a straight line and can be explained by a thermally activated transport of Arrhenius type:  $\sigma_{dc} = \sigma_0 exp(-E_a/k_BT)$ , where  $\sigma_0$ ,  $E_a$  and  $k_B$  represent the pre-exponential term, the activation energy of the mobile charge carriers and Boltzmann's constant, respectively. At lower temperature, a small deviation from the linear behavior of conductivity has been noticed and can be attributed to Mott's hopping type phenomena [37]. The dc activation energy of the material has been estimated to 0.002333eV.

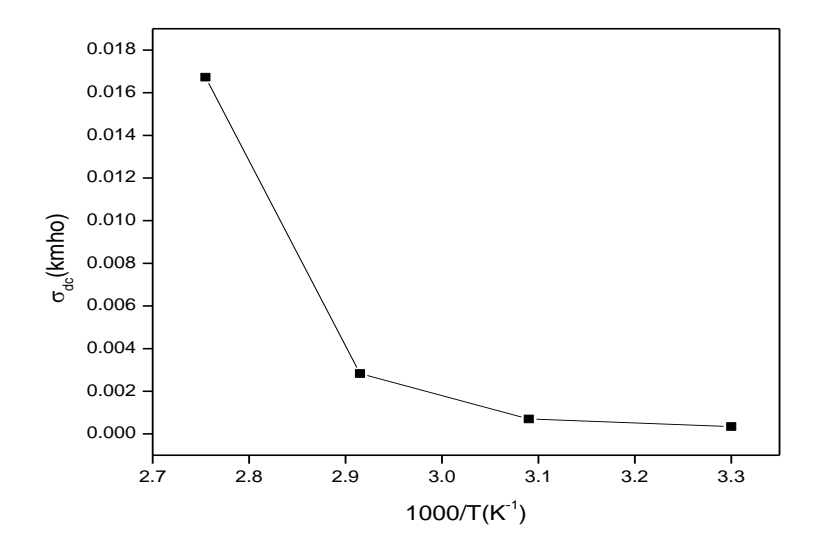


Figure 17: Variation of dc conductivity with inverse of temperature

# 5. Conclusion:

Optically good quality single crystal of gamma-glycine of size 7 x 5 x 3 mm<sup>3</sup> has been grown by slow evaporation technique at room temperature. The solubility of gamma-glycine crystal was estimated for water solvent at different temperatures. Single crystal XRD confirmed that the grown crystal belongs to the hexagonal system. The functional groups present in the crystal are confirmed by FTIR analysis. The optical transmittance spectral studies confirm that the crystals have very good transmittance in the entire visible region, with the lower UV cut-off around 241nm. The powder SHG test confirms that the efficiency of gamma-glycine is nearly 0.633 times as that of KDP crystals. Vickersmicro hardness value was calculated in order to understand the mechanical stability of the grown crystal. The thermal behavior of the crystals has been investigated by TGA analysis. The dielectric studies prove that the sample has low dielectric constant and dielectric loss values at high frequency. The real and imaginary parts of the impedance are found to be decreasing with increase of frequency for gamma-glycine crystal. From the Nyquist plot, the dc conductivity of the gamma-glycine crystal was calculated. The nonlinearity, transparency and thermal stabilities make this crystal suitable for SHG andopto-electronic device applications.

## **6.** Acknowledgments:

The authors are thankful to the supported work from the various research centers such as St.Joseph College (Trichy), M.K. University (Madurai), SAIF (Cochin), IISc (Bangalore). The authors are also grateful to the management of S.T. Hindu College, Nagercoil, Arignar Anna College, Aralvoymoli and the staff members of Sri Meenakshi Govt. Arts College for Women, Madurai.

### 7. References:

- 1. H.O. Marcy, L.F. Warren, M.S. Webb, C.A. Ebbers, S.P. Velsko, G.C. Kennedy, Appl.Opt., 1992, 31, 5051-5060.
- 2. S. Ledoux, J. Zyss, J. Int., Nonlinear Opt. Phys., 1994, 3, 287-316.
- 3. Y. Yukawa, Y. Inomata, T. Takeuchi, Bull.Chem. Soc. Jpn. 1983, 56, 2125-2128.
- 4. Y. Yukawa, N. Yasukawa, Y. Inomata, T.T akeuchi, Bull. Chem. Soc. Jpn., 1985, 58, 1591-1592.
- 5. B. Narayana Moolya, A. Jayaramo, M. R. Suresh Kumar, S. M. Dharmaprakash, J. Crystal growth 280 (2005) 581-590.
- 6. J. P. Legros, A. Kvick, Acta Crystallogr. B 36 (1980) 3052-3062.
- 7. T. N. Drebushchak, E. V. Boldyreva, E. S. Shutova, Acta Crystallogr. E 58(2002)634.

- 8. L. J. W. Shimon, M. Lahav, L. Leiserowitz, New J. Chem 10 (1986) 723.
- 9. B. Narayana Moolya, A. Jayaramo, M. R. Suresh Kumar, S. M. Dharmaprakash, J. Crystal growth 280 (2005) 581-590.
- 10. T. Balakrishnan, K. Ramamurthi, Cryst. Res. Technol. 2006, 41, 1184-1188.
- 11. M. Narayan Bhat, S.M. Dharmaprakash, J. Cryst Growth., 2002, 235, 511-516.
- 12. Ra. Shanmugavadivu, G. Ravi, A. Nixon Azariah, J. Phys. Chem. Solids. 2006, 67, 1858-1861.
- 13. T. Balakrishnan, K. Ramamurthi, Mater. Lett, 2008, 62, 65-68.
- 14. P. Selvarajan, J. Glorium, Arul Raj, S. Perumal, J. Cryst. Growth, 31(2009)3835-3840.
- 15. A. Shanthi, C. Krishnan, P. Selvarajan, Spectrochimica Acta Part A: Molecular and Bio molecular Spectroscopy 122 (2014) 521 528.
- 16. S. K. Kurtz, T. T. Perry, J. Appl. Phys, 39(1968)3798-3814.
- 17. H. Lipson, H. Steeple, Interpretation of X-Ray Powder Diffraction patterns, fifth ed. Macmillan, New York, 1970.
- 18. R. Sankar, C. M. Ragahvan, R. Mohan Kumar, R. Jayavel, J. Cryst Growth., 309 (2007) 30 36.
- 19. N. Vijayan, R. Ramesh Babu, R. Gopalakrishnan, S. Dhanushkodi, P. Ramasamy, J. Cryst. Growth, 236, 407 (2010).
- 20. S. G. Regith, C.Krishnan, Mater. Lett. 106 (2013) 87 89.
- 21. J. H. Westbrook, Report 58- RL-2033 of the G.E.Research Laboratory, USA, 1958.
- 22. W. Mott, Micro Indentation hardness Testing, Butterworth, London, 1956.
- 23. P. V. Raja Shekar, D. Nagaraju, V. Ganesh, K. Krishna Rao, Cryst. Res. Technol, 44 (2009) 652-656.
- 24. J. Mary Linet, S. Jerome Das, Physica B 405(2010)3955-3959.
- 25. B. Helina, P. Selvarajan, A. S. J. Lucia Rose, Phys. Scripta, 85 (2012) 055803-055808.
- 26. J. B. Charles, F. D, Gnanam, J. Matter. Sci. 29 (1993) 1395-1397.
- 27. E. Mayer, Z. Phys. 9(1908)66-74.
- 28. E. M. Onitsch, Mikroscopia, 2(1947) 131-151.
- 29. F. Q. Meng, M. K. L U, Z. H. Yang and H. Zeng, Matter. Lett. 33 (1998) 265.
- 30. P. Selvarajan, B. N. Das, H. B. Gon, K. V. Rao, J. Matter Sci, 29(1994) 4061-4064.
- 31. N. V. Prasad, G. Prasad, T. Bhimasankaran, S. V. Suryanarayana, G. S. Kumar, Indian J. Pure Appl. Phys, 34 (1996) 639-643.
- 32. C. Balarew, R. Dushlew, J. Solid State Chem, 55 (1984) 1 6.
- 33. K. V. Rao, A. Samukula, J. Appl. Phys, 36(1995)2031-2038.
- 34. A. S. J. Lucia Rose, P. Selvarajan, S. Perumal, Spectrochimica Acta Part A 81(2011)270-275.
- 35. J. Plocharski, W. Wieczoreck, Solid State Ionics 28-30 (1988) 979-982.
- 36. A. K. Jonscher, Nature 267 (1977) 673-679.
- 37. N. F. Mott, Metal Insulator Transitions, Taylor and Francis, London, 1990.